

Thermodynamic geometry and Joule-Thomson expansion of black holes in modified theories of gravity

Shahid Chaudhary,^{1,*} Abdul Jawad^{1,†} and Muhammad Yasir^{2,‡}

¹*Department of Mathematics, COMSATS University Islamabad, Lahore Campus-54000, Pakistan*

²*Department of Basic Sciences and Humanities, University of Engineering and Technology, Lahore (New Campus) 54890, Pakistan*

 (Received 11 July 2021; revised 22 November 2021; accepted 5 December 2021; published 11 January 2022)

The implication of Ruppeiner thermodynamic geometry theory to spherically symmetric black holes in anti-de Sitter (AdS) spacetime produces an unavoidable singularity in the line element of thermodynamic geometry. The singularity occurs due to the nonindependence of volume and entropy of black holes (BH) in AdS spacetime. In this work, we present an efficient and easy approach to deal the thermodynamic geometry of AdS BH in Einstein-Maxwell-scalars theory. We show that enthalpy instead of internal energy is central thermodynamic quantity. We develop the particular forms of the line element of thermodynamic geometry in different phase spaces. We find out that the curvatures in different phase spaces are identical and positive which leads to the repulsive interaction information between black hole molecules. We also analyze the thermal stability of AdS BH in Einstein-Maxwell-scalars theory and regularized Lovelock theory in the presence of thermal fluctuations. We observed that momentum relaxation parameter and coupling constants of Lovelock theory increase the thermal stability of the BHs. Finally, we also study the Joule-Thomson expansion for black hole in regularized Lovelock theory.

DOI: [10.1103/PhysRevD.105.024032](https://doi.org/10.1103/PhysRevD.105.024032)

I. INTRODUCTION

According to Boltzmann, if an object has temperature then it must possess microscopic structure, he proposed an adequate technique to decide whether the system has microstructure or not. Hawking and Bekenstein showed that a black hole (BH) has temperature and entropy on the event horizon, which confirms that it has microstructure [1,2]. The microstructure of BH has major significance in gravitation theory and BH physics. Recently, the hypothesis of a BH molecule [3] and the proposition of the thermodynamic geometry of BH [4–8] have promoted the study of microstructure of BH. The extended phase space with pressure P and volume V has attracted the interest of many researchers [9]. It has been shown that in extended phase space BHs show microstructure more abundantly [10–13]. The extended phase space can be introduced by interpreting the cosmological constant Λ as the thermodynamic pressure P , $P = \frac{-\Lambda}{8\pi} = \frac{3}{8\pi l^2}$ where l is the curvature radius.

The difference between the thermodynamic properties of BHs in AdS spacetime like Reissner Nordström (RN)-AdS BH, Gauss-Bonnet (GB) AdS BH, and Schwarzschild AdS BH etc, and the ordinary thermodynamic systems is that the heat capacity at constant volume becomes zero for BHs in AdS spacetime while this does not happen for the ordinary

thermodynamic systems. The reason for the zero specific heat is the non independence of entropy S and volume V of these BHs. One should be very careful when applying Ruppeiner thermodynamic geometry (RTG) theory to this kind of BH systems. The vanishing heat capacity at constant volume makes the line element of RTG singular, which produces divergence and it leads to the loss of information of the associated BH. The normalized curvature is used to fix this problem, which brings the heat capacity at constant volume extremely close to zero but not quite zero. Singh *et al.* [14] studied the thermodynamic curvature of AdS BHs with dark energy. They showed that dark energy significantly alters the BH microstructures. Small Schwarzschild-AdS BHs have attractive interactions while larger BHs have repulsive interactions which arise due to dark energy. The microscopic structures of many AdS BHs including RN and GB have been studied in literature works through the normalized curvature [15–17].

In this work, we use another more efficient method for the natural solution of singularity problem in the line element of RTG. This is the most effective technique for BHs in the AdS spacetime. We start with the basic and useful thermodynamic differential relation for AdS BH, $dM = TdS + VdP$. Using this basic relation for AdS BH we find out the line element of RTG for AdS BH in Einstein-Maxwell-scalars theory and the particular phase spaces (T, P) , (S, P) , (T, V) and (S, V) .

The corrected thermodynamics is very useful for the study of $P - V$ criticality, holographic duality and Joule

*shahidpeak00735@gmail.com

†abduljawad@cuilahore.edu.pk, jawadab181@yahoo.com

‡yasirciitsahawal@gmail.com

Thomson expansion of the BHs. In background of matter field corrected thermodynamics of BHs and the impact of thermal corrections on charged AdS BHs have shown significant results [18–20]. The quantum approach to thermodynamics of BHs is inevitable which required corrections in thermodynamical quantities. Frolov *et al.* [21] discussed the quantum corrections for the first time. According to them, the quantum gravity influences the entropy area relationship which leads to $S = S_o + \xi \log A + \eta_1 A^{-1} + \eta_2 A^{-2} \dots$, where $\xi, \eta_1, \eta_2, \dots$, are coefficients which depend upon BHs parameters [22]. Nozari *et al.* [23], also studied the influence of quantum corrections on the thermodynamics of BH.

Moradpour *et al.*, [24] discussed BHs solutions and Euler equation in modified theories of gravity. Moradpour *et al.*, [25] proposed dynamic BHs and by using Lematre metrics they provided physical properties of the BHs. Moradpour *et al.*, [26] derived the third law of thermodynamics for Schwarzschild BH. Nashed and Bamba [27] showed that energy conditions in Taub-NUT spacetime hold for charged BH. They also showed that charged (A)dS BHs in conformal teleparallel are equivalent of general relativity [28]. Ali *et al.*, [29] evaluated the impact of quantum gravity on stability of the BHs and proved that temperature depend on geometry and quantum gravity. Nashed and Bamba [30] found out the rotating BHs in quadratic $f(R)$ theory.

Recently new asymptotically AdS BH solutions in the Einstein-Maxwell-scalar theory have been constructed [31]. The Einstein-Maxwell-scalar theory has significant role in context of Kaluza-Klein models [32], cosmology [33] and supergravity/string theory [34]. In the past two years, the spontaneous scalarization of charged BHs has been discovered which motivated the number of studies on many Einstein-Maxwell-scalar models [35–37]. The importance of these models in recent researches motivate us to study Ruppeiner thermodynamic geometry and corrected thermodynamics of BHs in Einstein-Maxwell-scalar theory.

Joule-Thomson (JT) expansion is an important phenomenon in BH physics which deals with the study of change of temperature of a gas or fluid under adiabatical expansion. The JT coefficient U_{JT} finds out the change of temperature which can be positive or negative depend upon the fluid whether it is cooling or heating. In JT expansion gas at higher pressure goes through a porous plug to a section with a low pressure. A very important process during the expansion is the division of T - P plane in cooling and heating phase with the help of inversion temperature. The detail study of the isenthalpic and inversion curves for the case of Kerr-AdS BHs has been discussed in literature [38]. Chabab *et al.* [39], studied JT expansion for Reissner-Nordstrom BHs in AdS spacetimes. Recently JT expansion has been discussed for many BH solutions including arbitrary dimensional charged AdS BH [40,41],

Gauss-Bonnet AdS BHs [42] and nonlinear electrodynamic gravity. In Refs. [43,44], the JT effect of charged BH in rainbow gravity and the JT effect in AdS BH with momentum relaxation have been discussed.

Konoplya and Zhidenk generalizes the arbitrary Lovelock theory and proposed regularized Lovelock theory [45]. They discussed the charged static black objects in the Lovelock theory with both positive or negative cosmological constant curvature. They showed that metrics describe the four dimensional, charged asymptotically flat, dS and AdS BHs in the theory. Higher dimensional BH in the generalized Lovelock gravity has gained a lot of intentions recently [46]. Jawad and his collaborators have investigated thermal stability with modified gravity, accretion process and thermal fluctuations of some well-known black holes [47–52]. The importance of these BH in recent works motivates us to study temperature change of these BH through the well known process of JT expansion.

This paper is arranged as follows: In Sec. II, we explain RTG for AdS BH in Einstein-Maxwell-scalars theory. In Sec. III, we investigate thermal corrections of BH in Einstein-Maxwell-scalars theory. In Sec. IV, we study Joule-Thomson expansion for BH in regularized Lovelock theory. In Sec. V, we summarize our results in the conclusion.

II. RUPPEINER THERMODYNAMIC GEOMETRY

The RTG introduces a new method for extracting microscopic interaction information from thermodynamic axioms [53–55]. The total entropy of the isolated system including environment's entropy S_e (as an extensive infinite thermodynamic system) and the BH's entropy S is $S_{\text{total}} = S + S_e$. The X^μ correspond to extensive variables like mass M , angular momentum J , charge Q , etc of the BH and X_e^μ are extensivities for the environment. $\Delta X^\mu = X^\mu - X_0^\mu$ represents the difference of X^μ and its equilibrium value X_0^μ . As the isolated thermodynamic system yields local maximum entropy in equilibrium state. Thus, for small fluctuations ΔX^μ and ΔX_e^μ from the equilibrium, we can write change in total entropy as follows [56–58]

$$\begin{aligned} \Delta S_{\text{total}} = & \frac{\partial S}{\partial X^\mu} \Delta X^\mu + \frac{\partial S_e}{\partial X_e^\mu} \Delta X_e^\mu + \frac{1}{2} \frac{\partial^2 S}{\partial X^\mu \partial X^\nu} \Delta X^\mu \Delta X^\nu \\ & + \frac{1}{2} \frac{\partial^2 S_e}{\partial X_e^\mu \partial X_e^\nu} \Delta X_e^\mu \Delta X_e^\nu + \dots \end{aligned} \quad (1)$$

Due to law of conservation $\Delta X^\mu = -\Delta X_e^\mu$ and maximum entropy must be $\frac{\partial S}{\partial X^\mu} = \frac{\partial S_e}{\partial X_e^\mu}$. Considering the fact that environment is very large such that $S \ll S_e \approx S_{\text{total}}$, second quadratic term in the above equation can be neglected as compare to first one. Because the order of entropy S_e is same as the whole system, so the second derivatives with respect to X^μ are very much lesser than S . Thus, the above equation by ignoring the second term turns out to be

$$\Delta S_{\text{total}} = -\frac{1}{2}\Delta l^2, \quad \Delta l^2 = -\frac{\partial^2 S}{\partial X^\mu \partial X^\nu} \Delta X^\mu \Delta X^\nu. \quad (2)$$

From the above equation, one can say that the entropy as a thermodynamic potential yields thermodynamic line element as similar to the geometric one, which directly provides Ricci curvature scalar R . The thermodynamic geometry is basically based on the Riemannian geometry and its line element is defined as follows [56]

$$\Delta l^2 = -\frac{\partial^2 S}{\partial X^\mu \partial X^\nu} \Delta X^\mu \Delta X^\nu = -\Delta Y_\mu \Delta X^\mu, \quad (3)$$

$R = 0$ yields sign changing curvature while $R = \infty$ provides the critical points of phase transitions [59]. Although, we know that the positive/negative curvature corresponds to repulsive/ attractive microscopic interaction is still an open problem but it has been verified [56–58]. As BHs have temperature and entropy so they must have microstructure, but due impact of quantum gravity, some assumptions must be made while studying the microscopic features of BHs. The recent research works [60–64] have shown that based on well-established BH thermodynamics, the above thermodynamics geometry appears to be a plausible approach for extracting information about BH interactions. Hence, we employ this technique to study the properties of charged BH in Einstein-Maxwell-scalars theory.

A. AdS black hole in Einstein-Maxwell-Scalars theory

Andrade and Withers [31] studied Einstein-Maxwell-scalars gravity theory by homogeneously distributing 2 massless scalar fields with horizon coordinates. The action of the proposed model in 4 dimensions is given by

$$S_0 = \frac{1}{16\pi G} \int d^d x \sqrt{-g} \left[R - 2\Lambda - \frac{1}{4} F_{\mu\nu} F^{\mu\nu} - \frac{1}{2} \sum_{I=1}^2 (\partial\psi_I)^2 \right]. \quad (4)$$

Here $l^2 = -3/\Lambda$ is the relationship of cosmological and AdS radius. We have used the field strength $F = dA$ for a $U(1)$ gauge field A and the 2 massless scalar fields ψ_I . We set units such that gravitational constant satisfies $16\pi G = 1$. Using space-time with a planar base manifold and taking scalar fields to depend on the 2 dimensional spatial coordinates, the corresponding charged BH solution and the Klein-Gordon equation can easily be obtained as follows

$$ds^2 = -f(r)dt^2 + (f(r))^{-1}dr^2 + r^2 dx^a dx^a, \quad (5)$$

$$A = A_I(r)dt, \quad \psi_I = \beta_{Ia} x^a,$$

where a is the 2 spatial x^a directions, I is an internal index that represents the 2 scalar fields, and β_{Ia} are arbitrary real

constants. One can verify the following $f(r)$ for the above solution

$$f(r) = \frac{r^2}{l^2} - \frac{\beta^2}{2} - \frac{m}{r} + \frac{q^2}{r^2}, \quad A_I = \left(1 - \frac{r_0}{r}\right) \frac{2q}{r_0},$$

$$\beta^2 \equiv \frac{1}{2} \sum_{a=1}^2 \vec{\beta}_a \cdot \vec{\beta}_a \quad (6)$$

provided $\vec{\beta}_a \cdot \vec{\beta}_b = \beta^2 \delta_{ab} \forall a, b$. Here, we have introduced the vector notation $(\vec{\beta}_a)_I = \beta_{Ia}$ and $\vec{\beta}_a \cdot \vec{\beta}_b = \sum_I \beta_{Ia} \beta_{Ib}$. These and related solutions have previously been explored in [65], additionally see [66] for anisotropic examples with a single scalar. m and q are mass and charge, the index a goes to $a = 1, 2$, and the horizon radius r_0 satisfies $f(r_0) = 0$. In boundary theory, the linear coefficient β of scalar fields is used to define the strength of momentum relaxation [67]. The first law of thermodynamics for the charged BH is $dM = TdS + VdP + \phi dQ$, where the mass and temperature for the considered BH are given by

$$M = \frac{Pr_0^3}{3} + \frac{q^2}{8\pi r_0} - \frac{\beta^2 r_0}{16\pi},$$

$$T = -2 \left(-P + \frac{\beta^2}{16\pi r_0^2} + \frac{q^2}{8\pi r_0^4} \right) r_0. \quad (7)$$

The relations for pressure, thermodynamic volume, potential, and entropy for BH in Einstein-Maxwell-scalars gravity theory can be obtained as follows [68]

$$P = \frac{T}{2r_0} + \frac{\beta^2}{16\pi r_0^2} + \frac{q^2}{8\pi r_0^4}, \quad (8)$$

$$V = \frac{r_0^3}{3}, \quad (9)$$

$$\phi = \frac{q}{4\pi r_0}, \quad (10)$$

$$S = \frac{\pi r_0^2}{4}. \quad (11)$$

Basic and useful thermodynamic differential relation for AdS BH is $dM = TdS + VdP$. One can easily rewrite it as follows [68]

$$dS = \frac{1}{T} dM - \frac{V}{T} dP. \quad (12)$$

Considering S as thermodynamic potential, M and P can be assumed as extensive variables. We use $X^\mu = (M, P)$ and the intensive variables for X^μ becomes $Y_\mu = \partial S / \partial X^\mu = (1/T, -V/T)$. This yield an isolated system of BH and environment with same volume and temperature, where we have $M_{\text{total}} = M + M_e$ and $P_{\text{total}} = P + P_e$. The specific

form of each components in Eq. (3) provides the following relations

$$\begin{aligned}\Delta Y_0 &= \Delta\left(\frac{1}{T}\right) = -\frac{1}{T^2}\Delta T, \\ \Delta Y_1 &= \Delta\left(\frac{-V}{T}\right) = \frac{V}{T^2}\Delta T - \left(\frac{1}{T}\right)\Delta V.\end{aligned}\quad (13)$$

From the relation $\Delta M = T\Delta S + V\Delta P$, one can easily obtain the final form of the line element

$$\Delta l^2 = \frac{1}{T}\Delta T\Delta S + \frac{1}{T}\Delta V\Delta P. \quad (14)$$

According to first law of thermodynamics there are four coordinates spaces, which are $\{S, P\}$, $\{T, V\}$, $\{S, V\}$ and $\{T, P\}$. In coordinate space $\{S, P\}$, we can write

$$\begin{aligned}\Delta T &= \left(\frac{\partial T}{\partial P}\right)_P \Delta S + \left(\frac{\partial T}{\partial P}\right)_S \Delta P, \\ \Delta V &= \left(\frac{\partial V}{\partial S}\right)_P \Delta S + \left(\frac{\partial V}{\partial P}\right)_S \Delta P.\end{aligned}\quad (15)$$

Using the above relations into the Eq. (14), one can easily find out the following major equation [68]

$$\begin{aligned}\Delta l^2 &= \frac{1}{T}\left(\frac{\partial T}{\partial S}\right)_P \Delta S^2 + \frac{2}{T}\left(\frac{\partial T}{\partial P}\right)_S \Delta S\Delta P + \frac{1}{T}\left(\frac{\partial V}{\partial P}\right)_S \Delta P^2, \\ &= g_{\mu\nu}\Delta x^\mu\Delta x^\nu (x^\mu = S, P),\end{aligned}\quad (16)$$

where we have utilized the Maxwell relation $(\partial T/\partial P)_S = (\partial V/\partial S)_P$, which is based on relation $dM = TdS + VdP$. The differential equation of internal energy $dU = TdS - PdV$ along with Maxwell relation $(\partial T/\partial V)_S = -(\partial P/\partial S)_V$ leads to the line element in coordinate space $\{S, V\}$, given by

$$\begin{aligned}\Delta l^2 &= \frac{1}{T}\left(\frac{\partial T}{\partial S}\right)_V \Delta S^2 + \frac{1}{T}\left(\frac{\partial P}{\partial V}\right)_S \Delta V^2, \\ &= g_{\mu\nu}\Delta x^\mu\Delta x^\nu (x^\mu = S, V).\end{aligned}\quad (17)$$

Similarly, the Helmholtz free energy $dF = -SdT - PdV$ and the Maxwell relation $(\partial S/\partial V)_T = (\partial P/\partial T)_V$ provides the line element in coordinate space $\{T, V\}$ [68]

$$\begin{aligned}\Delta l^2 &= \frac{1}{T}\left(\frac{\partial S}{\partial T}\right)_V \Delta T^2 + \frac{2}{T}\left(\frac{\partial S}{\partial V}\right)_T \Delta T\Delta V + \frac{1}{T}\left(\frac{\partial P}{\partial V}\right)_S \Delta V^2, \\ &= g_{\mu\nu}\Delta x^\mu\Delta x^\nu (x^\mu = T, V).\end{aligned}\quad (18)$$

The line element in coordinate space $\{T, P\}$ by using Gibbs free energy $dG = -SdT + VdP$ and the Maxwell relation $(\partial S/\partial P)_T = -(\partial V/\partial T)_P$, turns out to be

$$\begin{aligned}\Delta l^2 &= \frac{1}{T}\left(\frac{\partial S}{\partial T}\right)_P \Delta T^2 + \frac{1}{T}\left(\frac{\partial V}{\partial P}\right)_T \Delta P^2, \\ &= g_{\mu\nu}\Delta x^\mu\Delta x^\nu (x^\mu = T, P).\end{aligned}\quad (19)$$

The line element of thermodynamic geometry in the $\{S, q\}$ space takes the following form

$$\begin{aligned}\Delta l^2 &= \frac{1}{T}\left(\frac{\partial T}{\partial S}\right)_q \Delta S^2 + \frac{2}{T}\left(\frac{\partial T}{\partial q}\right)_S \Delta S\Delta q + \frac{1}{T}\left(\frac{\partial \phi}{\partial q}\right)_S \Delta q^2, \\ &= g_{\mu\nu}\Delta x^\mu\Delta x^\nu (x^\mu = S, q).\end{aligned}\quad (20)$$

Due to the Legendre transformation between the thermodynamic potential functions, one can say that the curvatures created by the five line elements are comparable. Now, we are able to apply the above mentioned coordinate spaces to AdS BH in Einstein-Maxwell-scalars theory. Using Eq. (8) for largest positive horizon into Eqs. (11) and (9) yields the following relations

$$S = \frac{1}{64} \frac{2T^2\pi - 2T\sqrt{\pi}\sqrt{T^2\pi + P\beta^2} + P\beta^2}{P^2\pi}, \quad (21)$$

$$V = \frac{2\sqrt{2}\sqrt{3}q^3P^{3/2}}{(2T^2\pi - 2T\sqrt{\pi}\sqrt{T^2\pi + P\beta^2} + P\beta^2)^{3/2}}. \quad (22)$$

Now from Eq. (19), we can obtain the expression of thermodynamic curvature

$$\begin{aligned}R_{\text{TP}} &= \frac{8}{9}\sqrt{3P}\left(24T^2\left(\frac{1}{64}\frac{2T^2\pi - 2T\sqrt{\pi}\sqrt{T^2\pi + P\beta^2} + P\beta^2}{P^2\pi}\right)^2\pi^{3/2}P^4\beta^8\right. \\ &\quad + 6\beta^6P^{9/2}(T^2\pi + P\beta^2)^{\frac{1}{2}}q^3\sqrt{6\left(\frac{1}{64}\frac{2T^2\pi - 2T\sqrt{\pi}\sqrt{T^2\pi + P\beta^2} + P\beta^2}{P^2\pi}\right)\pi} \\ &\quad - 18\beta^6P^{9/2}Tq^3\pi\left(6\left(\frac{1}{64}(2T^2\pi - 2T\sqrt{\pi}\sqrt{T^2\pi + P\beta^2} + P\beta^2)(P^2\pi)^{-1}\right)\right)^{\frac{1}{2}} + 444\beta^6P^3T^4(164/((2T^2\pi - 2T\sqrt{\pi} \\ &\quad \times (T^2\pi + P\beta^2)^{\frac{1}{2}} + P\beta^2)(P^2\pi)^{-1}))^2\pi^{5/2} - 152\beta^6P^3\sqrt{T^2\pi + P\beta^2}((2T^2\pi - 2T\sqrt{\pi}\end{aligned}$$

$$\begin{aligned}
& \times \sqrt{(T^2\pi + P\beta^2 + P\beta^2)/(64P^2\pi)} T^3\pi^2 - 54\beta^4 P^{7/2} q^3 \pi^2 [3((2T^2\pi - 2T\sqrt{\pi}[T^2\pi + P\beta^2])^{\frac{1}{2}} \\
& + P\beta^2)/32P^2\pi)]^{\frac{1}{2}}/T^3 + 33\beta^4 P^{7/2} \sqrt{(T^2\pi + P\beta^2)q^3\sqrt{2}\sqrt{3}} \left[(2T^2\pi - 2T\sqrt{\pi} \right. \\
& \times \sqrt{(T^2\pi + P\beta^2 + P\beta^2)/(64P^2\pi)} \left. \right]^{\frac{1}{2}} \pi^{3/2} T^2 - 776\beta^4 P^2 [(2T^2\pi - 2T\sqrt{\pi}[T^2\pi + P\beta^2])^{\frac{1}{2}} \\
& + P\beta^2)/64P^2\pi]^2 T^5 \pi^3 + 1208\beta^4 P^2 T^6 [3((2T^2\pi - 2T\sqrt{\pi}[T^2\pi + P\beta^2])^{\frac{1}{2}} + P\beta^2) \\
& \times /32P^2\pi)]^2 \pi^{7/2} + 45\beta^2 P^{5/2} \sqrt{(T^2\pi + P\beta^2)q^3\sqrt{2}\sqrt{3}} [(2T^2\pi - 2T\sqrt{\pi}[T^2\pi + P\beta^2])^{\frac{1}{2}} \\
& + P\beta^2)/64P^2\pi]^2 \pi^{5/2} T^4 - [((2T^2\pi - 2T\sqrt{\pi}[T^2\pi + P\beta^2])^{\frac{1}{2}} + P\beta^2)/64P^2\pi]^{\frac{1}{2}} \\
& \times [54\beta^2 \times P^{5/2} q^3 \pi^3 \sqrt{2}\sqrt{3}/T^5 - 18P^{3/2} q^3 \pi^4 \sqrt{2}\sqrt{3} T^7 + 18P^{3/2} \sqrt{(T^2\pi + P\beta^2)q^3\sqrt{2}\sqrt{3}\pi^{7/2} T^6} \\
& + [((2T^2\pi - 2T\sqrt{\pi}[T^2\pi + P\beta^2])^{\frac{1}{2}} + P\beta^2)/64P^2\pi]^2] [1152\beta^2 P T^8 \pi^{9/2} - 960\beta^2 P \\
& \times [T^2\pi + P\beta^2]^{\frac{1}{2}} T^7 \pi^4 - 384\sqrt{(T^2\pi + P\beta^2)}] + 384T^{10} \pi^{11/2} \pi \sqrt{2}/[(2T^2\pi - 2, T\sqrt{\pi}[T^2\pi + P\beta^2])^{\frac{1}{2}} \\
& + P\beta^2)/64P^2\pi]^2 (T^2\pi + P\beta^2)^2 (-2T\pi \sqrt{(T^2\pi + P\beta^2)} + 2T^2 \pi^{3/2} + \sqrt{\pi} P \beta^2)^2 T q^3. \tag{23}
\end{aligned}$$

For the space $\{S, P\}$, Eqs. (7), (9), and (11) yields temperature T and volume V in terms of entropy S and pressure P as follow

$$T = -4 \left(-P + \frac{1}{64} \frac{\beta^2}{\pi S} \right) \sqrt{S}, \quad V = \frac{\sqrt{6} q^3}{256 P^{3/2} S^{3/2} \pi^{3/2}}.$$

Finally by using Eq. (16), the thermodynamic curvature corresponding to these relations takes the following form

$$\begin{aligned}
R_{SP} = & 128 \left(P\pi S \left(16384 P^2 \pi^2 S^4 + 6S\beta^2 \left(1/3 \left(\sqrt{-6\beta^2 S - 384 P \pi S^2} \right) \right)^2 + 768\beta^2 P \pi S^3 \right. \right. \\
& + 512 P \pi S^2 \left(1/3 \left(\sqrt{-6\beta^2 S - 384 P \pi S^2} \right) \right)^2 + 3q^4 \left. \right) (2\beta^2 S + (1/3((-6\beta^2 S - 384 \\
& \times P \pi S^2)^{\frac{1}{2}}))^2 + 128 P \pi S^2)^2 (128 P \pi S^2 - 2\beta^2 S - \left(1/3 \left(\sqrt{-6\beta^2 S - 384 P \pi S^2} \right) \right)^2). \tag{24}
\end{aligned}$$

For the coordinate space $\{T, V\}$ and $\{S, V\}$, the analytical relations are very lengthy and we have not shown here. One can verify that $R_{TP} = R_{SP}$ and we also verified the identity $R_{TP} = R_{SP} = R_{TV} = R_{SV}$. Moreover, for the extreme BH $T = 0$, the curvature becomes positive. Based on the standard result, positive-negative thermodynamic curvature is related with the repulsive-attractive microscopic interactions, we can conclude that molecules of BH in Einstein-Maxwell-scalars theory show repulsion. In addition with no AdS background $P = 0$ curvature becomes zero which represents that the BH in Einstein-Maxwell-scalars theory with no AdS background is Ruppeiner flat.

III. THERMAL CORRECTIONS OF BLACK HOLE IN EINSTEIN-MAXWELL-SCALARS THEORY

The corrections to thermodynamics of BHs has become a frequent subject of study and it has gained a prominent

place in BH physics. It is used to discuss stability/instability, criticality, phase transitions and many other features of BHs. In this section, we study various thermodynamic quantities like corrected entropy, Helmholtz free energy, internal energy, pressure, enthalpy, and Gibbs free energy of BH in Einstein-Maxwell-scalars theory. According to area law, the entropy of the BH is defined as $S = A/4$, where A is the area of horizon. The quantum corrections alter the manifold structure near the Planck scale which changes the holographic principle. This leads to the change in area law of BH entropy. The modified entropy-area law takes the following form [20–21]

$$S_c = S - (b/2) \ln(ST^2). \tag{25}$$

Utilizing the values of S and T , the corrected entropy of BH in Einstein-Maxwell-scalars theory turns out to be

$$S_c = \pi r_0^2 - b/2 \ln \left(4\pi r_0^4 \left(-P + \frac{\beta^2}{16\pi r_0^2} + \frac{q^2}{8\pi r_0^4} \right)^2 \right). \quad (26)$$

Helmholtz free energy is the useful thermodynamical quantity which find out work done by the system. Helmholtz free energy can be calculated from $F = M - TS_c$. Using mass, temperature and the corrected entropy of the BH, it turns out to be

$$F = \frac{Pr_0^3}{3} + \frac{q^2}{8\pi r_0} - \frac{\beta^2 r_0}{16\pi} + 2 \left(-P + \frac{\beta^2}{16\pi r_0^2} + \frac{q^2}{8\pi r_0^4} \right) r_0 \left(\pi r_0^2 - \frac{b}{2} \ln \left(4\pi r_0^4 \left(-P + \frac{\beta^2}{16\pi r_0^2} + \frac{q^2}{8\pi r_0^4} \right)^2 \right) \right). \quad (27)$$

The internal energy of BH in Einstein-Maxwell-scalars theory can be calculated from $E = F + TS_c$ and it becomes

$$E = \frac{16\pi^2 r_0^6 P + ((-3\beta^2 - 48bP)r_0^4 + 6r_0^2 q^2)\pi + 2bq^2}{12\pi r_0^3}. \quad (28)$$

Another significant thermodynamical quantity is enthalpy which is used to evaluate the change in energy of the system. One can obtain the enthalpy by using $H = E + PV$, which leads to the following form

$$H = \frac{-4\pi\Lambda r_0^6 - 6\pi\beta^2 r_0^4 + 12b\Lambda r_0^4 + 4bq^2 + 12\pi q^2 r_0^2 - \Lambda r_0^6}{24\pi r_0^3}. \quad (29)$$

Figures 1 and 2 show the behavior of Helmholtz free energy versus r_o for different values of momentum relaxation parameter β and correction coefficient b . One can see from the plot that Helmholtz free energy increases with increasing values of momentum relaxation parameter β , which mean more work can be extracted from the system for higher values of parameter β . For small BHs the Helmholtz free energy is low while for large BHs it is high. For the case $\beta = 0$, the Helmholtz free energy remains zero which show equilibrium state and no further work can be obtained without momentum relaxation. Figure 2 shows the influence of correction coefficient b . The Helmholtz free energy remains negative throughout the range of r_o for all the values of correction coefficient.

A. Thermal stability

The amount of heat required to change the temperature of a BH is called heat capacity or thermal capacity. There are

two categories to measure the heat capacity, one is specific heat at constant pressure in which heat is added to system at constant pressure while the other is specific heat at constant volume, which measure the heat when it is added to system at constant volume. One can obtain the specific heat at the constant volume by using the following relation

$$C_V = T \left(\frac{\partial S_c}{\partial r} \right) \left(\frac{\partial r}{\partial T} \right). \quad (30)$$

Using the relations of entropy and temperature, one can easily obtain the specific heat for BH in Einstein-Maxwell-scalars theory, given by

$$C_V = \frac{-2\pi r_0^4 (16bP + \beta^2) - 4bq^2 + 32\pi^2 P r_0^6 - 4\pi q^2 r_0^2}{\beta^2 r_0^2 + 16\pi P r_0^4 + 6q^2}. \quad (31)$$

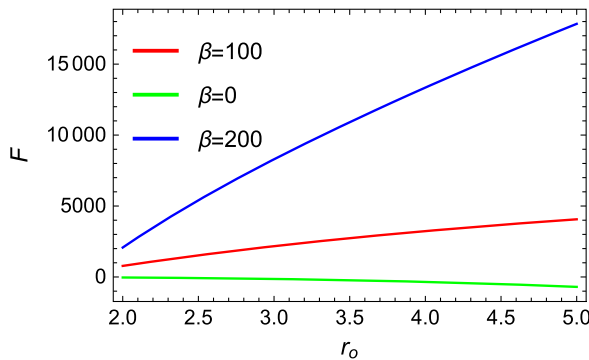


FIG. 1. Plot of Helmholtz free energy F versus r_o for BH in Einstein-Maxwell-scalars theory.

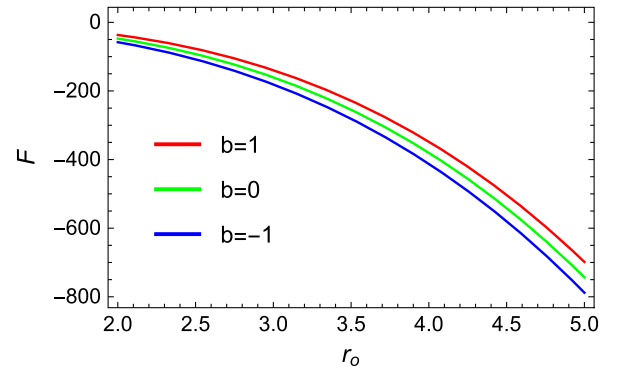


FIG. 2. Plot of Helmholtz free energy F versus r_o for BH in Einstein-Maxwell-scalars theory.

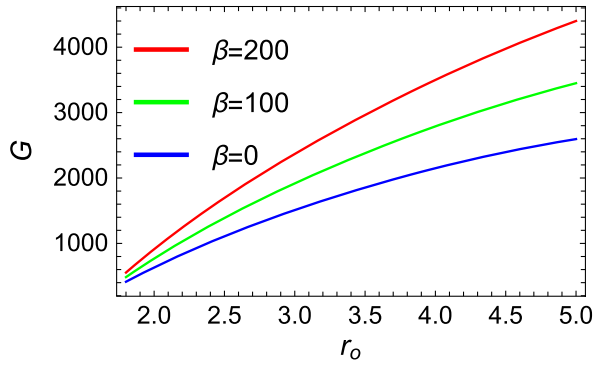


FIG. 3. Plot of Gibbs free energy G versus r_o for BH in Einstein-Maxwell-scalars theory.

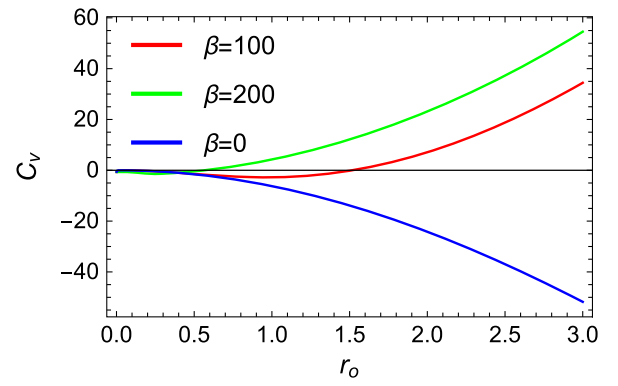


FIG. 5. Plot of specific heat C_V versus r_o for BH in Einstein-Maxwell-scalars theory.

In canonical ensemble, the free energy is known as the Gibbs free energy by using $G = M - TS_c + PV$, the relation for Gibbs free energy turns out to be

$$G = \left(-3b(\beta^2 r^2 - 16\pi P r^4 + 2q^2) \log \left(\frac{(\beta^2 r^2 - 16\pi P r^4 + 2q^2)^2}{64\pi r^4} \right) + 2r^4((3\pi - 1)\beta^2 + 4\pi r(2(1 - 6\pi)Pr + T)) + 4(2 + 3\pi)q^2 r^2 \right) (48\pi r^3)^{-1}.$$

Figures 3 and 4 show the Gibbs free energy of BH in Einstein-Maxwell-scalars theory for different values of momentum relaxation parameter β and correction coefficient b respectively. In Fig. 3 the positive Gibbs energy corresponds to nonspontaneous reactions which occurs with outside source of energy while the negative Gibbs energy in Fig. 4 corresponds to spontaneous reactions which occurs without any outside source of energy. BHs with negative Gibbs free energy are thermodynamically unstable and they release energy in the surroundings to get the low energy state. For all the values of momentum relaxation parameter β , the Gibbs free energy is positive which show global stability while for all the values (positive and negative) of correction coefficient b , the Gibbs free energy is negative which show global instability.

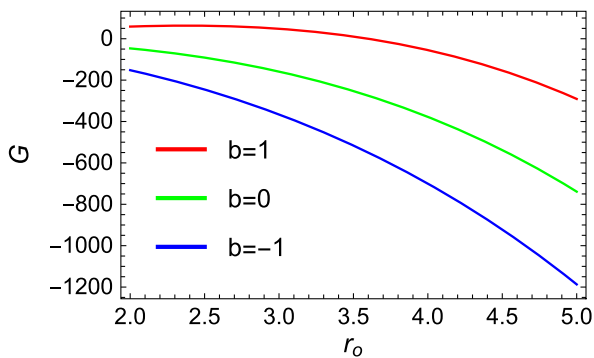


FIG. 4. Plot of Gibbs free energy G versus r_o for BH in Einstein-Maxwell-scalars theory.

Figures 5 and 6 demonstrate the behavior of specific heat for different values of momentum relaxation parameter β and correction coefficient b . Specific heat is used to discuss the local stability of BHs, $C_V > 0$ represents the local stability of BH while $C_V < 0$ shows the local instability. The influence of momentum relaxation parameter β is significant because it makes the BH stable. It can be seen that for the case $\beta = 0$ the BH becomes unstable due to negative specific heat. The negative correction coefficient $b = -1$ makes the specific heat more positive as compared to $b = 0, 1$ which means BH becomes more stable for negative correction coefficient. Small BH are locally unstable while large BHs becomes locally stable.

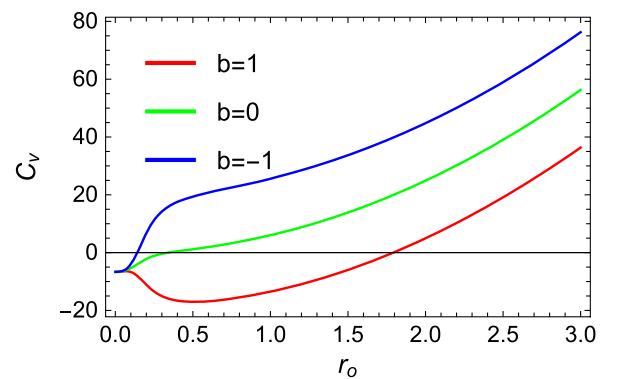


FIG. 6. Plot of specific heat C_V versus r_o for BH in Einstein-Maxwell-scalars theory.

IV. JOULE-THOMSON EXPANSION FOR BH IN REGULARIZED LOVELOCK THEORY

Glavan and Lin recently formulated 4D Einstein GB theory of gravity which is different from the pure Einstein theory [69]. The general form of D -dimensional static as well as maximally symmetric metric is given by

$$ds^2 = -f(r)dt^2 + (f(r))^{-1}dr^2 + r^2\gamma_{ij}dx^i dx^j, \quad (32)$$

where $d\Omega_n^2$ is $(n = D - 2)$ -dimensional constant curvature space with curvature $\kappa = -1, 0, 1$. $\kappa = 1$ represents spherically symmetric BH solution. For detail solution of the BH in regularized Lovelock theory see [70]. There exist two branches of $f(r)$ for $D = 4$, which are given by [70]

$$f(r) = 1 - \frac{\tilde{\alpha}_2 r^2}{3\tilde{\alpha}_3} (A_+(r) - A_-(r) - 1), \quad A_{\pm} = \sqrt[3]{\sqrt{F(r)^2 + \left(\frac{3\tilde{\alpha}_3}{\tilde{\alpha}_2^2} - 1\right)^3} \pm F(r)}, \quad (33)$$

where

$$F(r) = \frac{27\tilde{\alpha}_3^2}{2\tilde{\alpha}_2^3} \left(\frac{2M}{r^3} - \frac{Q^2}{r^4} + \frac{\Lambda}{3} \right) + \frac{9\tilde{\alpha}_3}{2\tilde{\alpha}_2^2} - 1, \quad (34)$$

$\tilde{\alpha}_2$ and $\tilde{\alpha}_3$ are arbitrary constants of the theory. The higher-order Lovelock corrections yields more branches. However, there is always only one branch which is perturbative for $\tilde{\alpha}_3 \geq \frac{\tilde{\alpha}_2^2}{3}$ [70]. We study the case $\tilde{\alpha}_3 = \frac{\tilde{\alpha}_2^2}{3}$ in our work. Taking $f(r) = 0$ and solving the equation for M , the mass of BH in regularized Lovelock theory yields as

$$M = (8\pi(\tilde{\alpha}_2)^3(\tilde{\alpha}_3^2)Pr_0^6 + 3(\tilde{\alpha}_2)^3(\tilde{\alpha}_3^2)Q^2r_0^2 + (\tilde{\alpha}_2)^2(\tilde{\alpha}_3)(\tilde{\alpha}_2^3)r_0^4 + 3(\tilde{\alpha}_2)(\tilde{\alpha}_3)^2(\tilde{\alpha}_2^3)r_0^2 + 3(\tilde{\alpha}_3)^3(\tilde{\alpha}_2^3))/6(\tilde{\alpha}_2)^3(\tilde{\alpha}_3^2)r_0^3.$$

From the above equation, one can easily find the pressure of BH in terms of mass and charge as follows

$$P = (6(\tilde{\alpha}_2)^3(\tilde{\alpha}_3^2)Mr_0^3 - 3(\tilde{\alpha}_2)^3(\tilde{\alpha}_3^2)Q^2r_0^2 - (\tilde{\alpha}_2)^2(\tilde{\alpha}_3)(\tilde{\alpha}_2^3)r_0^4 - 3(\tilde{\alpha}_2)(\tilde{\alpha}_3)^2(\tilde{\alpha}_2^3)r_0^2 - 3(\tilde{\alpha}_3)^3 \times (\tilde{\alpha}_2^3))/8\pi(\tilde{\alpha}_2)^3(\tilde{\alpha}_3^2)r_0^6.$$

Another important thermal quantity is Hawking temperature $T = f'(r)/4\pi$ and for BH in regularized Lovelock theory it turns out to be

$$T = \left(2(\tilde{\alpha}_2) \left(r_0^4 \left((\tilde{\alpha}_2^3) \left(\left(\frac{r_0^4(\tilde{\alpha}_2^3 - 72\pi(\tilde{\alpha}_3^2)P) + 54(\tilde{\alpha}_3^2)Mr_0 - 27(\tilde{\alpha}_3^2)Q^2}{(\tilde{\alpha}_2^3)r_0^4} \right)^{2/3} - 1 \right) + 72\pi(\tilde{\alpha}_3^2)P \right) - 27(\tilde{\alpha}_3^2)Mr_0 + 9(\tilde{\alpha}_3^2)Q^2 \right) \right) (12\pi(\tilde{\alpha}_3) \left((r_0^3((\tilde{\alpha}_2^3) - 72\pi(\tilde{\alpha}_3^2)P) + 54(\tilde{\alpha}_3^2)M - 27(\tilde{\alpha}_3^2)Q^2r_0^{-1}) \right)^{2/3})^{-1}.$$

Using this temperature in Eq. (25), the first order corrected entropy of BH in regularized Lovelock theory becomes

$$S_c = \pi r_0^2 - \frac{1}{2} b \log \left(\left(\left(\tilde{\alpha}_2^3 r_0^2 \left(9\tilde{\alpha}_3^2 (Q^2 - 8\pi P r_0^4) - 2\tilde{\alpha}_2^3 r_0^4 \left(\left(\frac{(\tilde{\alpha}_2 r_0^2 + 3\tilde{\alpha}_3)^3}{\tilde{\alpha}_2^3 r_0^6} \right)^{2/3} - 1 \right) \right) + 9\tilde{\alpha}_2^2 \tilde{\alpha}_3 \tilde{\alpha}_2^3 r_0^4 + 27\tilde{\alpha}_2 \tilde{\alpha}_3^2 \tilde{\alpha}_2^3 r_0^2 + 27\tilde{\alpha}_3^3 \tilde{\alpha}_2^3 \right)^2 \right) (144\pi \tilde{\alpha}_2^4 \tilde{\alpha}_3^2 (\tilde{\alpha}_2^3)^2 r_0^8 \left(\frac{(\tilde{\alpha}_2 r_0^2 + 3\tilde{\alpha}_3)^3}{\tilde{\alpha}_2^3 r_0^6} \right)^{4/3})^{-1} \right).$$

The Helmholtz free energy for BH in regularized Lovelock theory takes the following form

$$F = \frac{2r_0^2(\tilde{\alpha}_2^2\tilde{\alpha}_3\tilde{\alpha}_2^3r_0^4 + \tilde{\alpha}_2^3\tilde{\alpha}_3^2r_0^2(8\pi Pr_0^4 + 3Q^2) + 3\tilde{\alpha}_2\tilde{\alpha}_3^2\tilde{\alpha}_2^3r_0^2 + 3\tilde{\alpha}_3^3\tilde{\alpha}_2^3)}{\tilde{\alpha}_3^2} - (\tilde{\alpha}_2(\tilde{\alpha}_2^3r_0^2(2\tilde{\alpha}_2^3r_0^4(((\tilde{\alpha}_2r_0^2 + 3\tilde{\alpha}_3)^3)(\tilde{\alpha}_2^3r_0^6)^{-1})^{2/3} - 1) \\ - 9\tilde{\alpha}_3^2(Q^2 - 8\pi Pr_0^4)) - 9\tilde{\alpha}_2^2\tilde{\alpha}_3\tilde{\alpha}_2^3r_0^4 - 27\tilde{\alpha}_2\tilde{\alpha}_3^2\tilde{\alpha}_2^3r_0^2 - 27\tilde{\alpha}_3^3\tilde{\alpha}_2^3)(\pi r_0^2 - \frac{1}{2}b \log\left(\left(\left(\tilde{\alpha}_2^3r_0^2\left(9\tilde{\alpha}_3^2(Q^2 - 8\pi Pr_0^4) \right. \right. \right. \right. \\ \left. \left. \left. - 2\tilde{\alpha}_2^3r_0^4\left(\left(\frac{(\tilde{\alpha}_2r_0^2 + 3\tilde{\alpha}_3)^3}{\tilde{\alpha}_2^3r_0^6}\right)^{2/3} - 1\right)\right)\right) + 9\tilde{\alpha}_2^2\tilde{\alpha}_3\tilde{\alpha}_2^3r_0^4 + 27\tilde{\alpha}_2\tilde{\alpha}_3^2\tilde{\alpha}_2^3r_0^2 + 27\tilde{\alpha}_3^3\tilde{\alpha}_2^3\right)^2 \\ \times \left(144\pi\tilde{\alpha}_2^4\tilde{\alpha}_3^2(\tilde{\alpha}_2^2)^2r_0^8\left(\frac{(\tilde{\alpha}_2r_0^2 + 3\tilde{\alpha}_3)^3}{\tilde{\alpha}_2^3r_0^6}\right)^{4/3}\right)^{-1}\left)\right)\left(\pi\tilde{\alpha}_3\tilde{\alpha}_2^3\left(\frac{(\tilde{\alpha}_2r_0^2 + 3\tilde{\alpha}_3)^3}{\tilde{\alpha}_2^3r_0^6}\right)^{2/3}\right)(12\tilde{\alpha}_2^3r_0^5)^{-1}$$

The Gibbs free energy for the considered model of the BH turns out to be

$$G = \left(\tilde{\alpha}_2\tilde{\alpha}_3^2b\left(\tilde{\alpha}_2^3r_0^2\left(2\tilde{\alpha}_2^3r_0^4\left(\left(\frac{(\tilde{\alpha}_2r_0^2 + 3\tilde{\alpha}_3)^3}{\tilde{\alpha}_2^3r_0^6}\right)^{2/3} - 1\right) - 9\tilde{\alpha}_3^2(Q^2 - 8\pi Pr_0^4)\right) - 9\tilde{\alpha}_2^2\tilde{\alpha}_3\tilde{\alpha}_2^3r_0^4 - 27\tilde{\alpha}_2 \\ \times \tilde{\alpha}_3^2\tilde{\alpha}_2^3r_0^2 - 27\tilde{\alpha}_3^3\tilde{\alpha}_2^3\right) \log\left(\left(\left(\tilde{\alpha}_2^3r_0^2\left(9\tilde{\alpha}_3^2(Q^2 - 8\pi Pr_0^4) - 2\tilde{\alpha}_2^3r_0^4\left(\left(\frac{(\tilde{\alpha}_2r_0^2 + 3\tilde{\alpha}_3)^3}{\tilde{\alpha}_2^3r_0^6}\right)^{2/3} - 1\right)\right) \right. \right. \right. \\ \left. \left. \left. + 9\tilde{\alpha}_2^2\tilde{\alpha}_3\tilde{\alpha}_2^3r_0^4 + 27\tilde{\alpha}_2\tilde{\alpha}_3^2\tilde{\alpha}_2^3r_0^2 + 27\tilde{\alpha}_3^3\tilde{\alpha}_2^3\right)^2\right)(144\pi\tilde{\alpha}_2^4\tilde{\alpha}_3^2(\tilde{\alpha}_2^2)^2r_0^8\left(\frac{(\tilde{\alpha}_2r_0^2 + 3\tilde{\alpha}_3)^3}{\tilde{\alpha}_2^3r_0^6}\right)^{4/3}\right)^{-1} \\ \left. + 2\pi r_0^2(6\tilde{\alpha}_3^4(\tilde{\alpha}_2^2)^2\left(\frac{(\tilde{\alpha}_2r_0^2 + 3\tilde{\alpha}_3)^3}{\tilde{\alpha}_2^3r_0^6}\right)^{2/3} + 3\tilde{\alpha}_2\tilde{\alpha}_3\tilde{\alpha}_2^3(2\tilde{\alpha}_2^3r_0^2\left(\frac{(\tilde{\alpha}_2r_0^2 + 3\tilde{\alpha}_3)^3}{\tilde{\alpha}_2^3r_0^6}\right)^{2/3} + 9\tilde{\alpha}_3^2) + \tilde{\alpha}_2^2\tilde{\alpha}_3^2 \right. \\ \times \tilde{\alpha}_2^3r_0^2\left(2\tilde{\alpha}_2^3r_0^2\left(\frac{(\tilde{\alpha}_2r_0^2 + 3\tilde{\alpha}_3)^3}{\tilde{\alpha}_2^3r_0^6}\right)^{2/3} + 27\tilde{\alpha}_3^2) + \tilde{\alpha}_2^3\tilde{\alpha}_3\tilde{\alpha}_2^3\tilde{\alpha}_3^2r_0^2\left(32\pi Pr_0^4\left(\frac{(\tilde{\alpha}_2r_0^2 + 3\tilde{\alpha}_3)^3}{\tilde{\alpha}_2^3r_0^6}\right)^{2/3} \right. \\ \left. \left. + 6Q^2\left(\frac{(\tilde{\alpha}_2r_0^2 + 3\tilde{\alpha}_3)^3}{\tilde{\alpha}_2^3r_0^6}\right)^{2/3} + 9r_0^2) + \tilde{\alpha}_2^4\tilde{\alpha}_3^2r_0^2\left(9\tilde{\alpha}_3^2(Q^2 - 8\pi Pr_0^4) - 2\tilde{\alpha}_2^3r_0^4\left(\left(\frac{(\tilde{\alpha}_2r_0^2 + 3\tilde{\alpha}_3)^3}{\tilde{\alpha}_2^3r_0^6}\right)^{2/3} - 1\right)\right)\right) \\ \times \left(24\pi\tilde{\alpha}_2^3\tilde{\alpha}_3\tilde{\alpha}_2^3\tilde{\alpha}_3^2r_0^5\left(\frac{(\tilde{\alpha}_2r_0^2 + 3\tilde{\alpha}_3)^3}{\tilde{\alpha}_2^3r_0^6}\right)^{2/3}\right)^{-1}$$

In order to discuss the local stability of the BH, the relation for specific heat by using Eq. (30), becomes

$$C_V = \left(2r_0^2(27\tilde{\alpha}_2^2\tilde{\alpha}_3^2\tilde{\alpha}_2^3r_0^2(b - 2\pi r_0^2) + \tilde{\alpha}_2^4\left(-\left(2\tilde{\alpha}_2^3r_0^6(b - \pi r_0^2)\left(\left(\frac{(\tilde{\alpha}_2r_0^2 + 3\tilde{\alpha}_3)^3}{\tilde{\alpha}_2^3r_0^6}\right)^{2/3} - 1\right) + 9\tilde{\alpha}_3^2 \right. \right. \right. \\ \times (br_0^2(8\pi Pr_0^4 + Q^2) + \pi r_0^4(Q^2 - 8\pi Pr_0^4))\right) + 3\tilde{\alpha}_2^3\tilde{\alpha}_3\left(-2\tilde{\alpha}_2^3br_0^4\left(\left(\frac{(\tilde{\alpha}_2r_0^2 + 3\tilde{\alpha}_3)^3}{\tilde{\alpha}_2^3r_0^6}\right)^{2/3} - 3\right) \right. \\ \left. \left. + \pi\tilde{\alpha}_2^3r_0^6\left(2\left(\frac{(\tilde{\alpha}_2r_0^2 + 3\tilde{\alpha}_3)^3}{\tilde{\alpha}_2^3r_0^6}\right)^{2/3} - 5\right) + 9\tilde{\alpha}_3^2b(Q^2 - 24\pi Pr_0^4) + 9\pi\tilde{\alpha}_2^3r_0^2(8\pi Pr_0^4 - Q^2)\right) + 27 \right. \\ \times \tilde{\alpha}_2\tilde{\alpha}_3^3\tilde{\alpha}_2^3(b - 4\pi r_0^2) - 81\pi\tilde{\alpha}_3^4\tilde{\alpha}_2^3\left.\right)\left(-3\tilde{\alpha}_2^3\tilde{\alpha}_3r_0^2\left(\tilde{\alpha}_2^3r_0^4\left(7 - 2\left(\frac{(\tilde{\alpha}_2r_0^2 + 3\tilde{\alpha}_3)^3}{\tilde{\alpha}_2^3r_0^6}\right)^{2/3}\right) + 9\tilde{\alpha}_3^2(Q^2 - 40\pi Pr_0^4)\right) \right. \\ \left. \left. + \tilde{\alpha}_2^4r_0^4(2\tilde{\alpha}_2^3r_0^4\left(\left(\frac{(\tilde{\alpha}_2r_0^2 + 3\tilde{\alpha}_3)^3}{\tilde{\alpha}_2^3r_0^6}\right)^{2/3} - 1\right) + 9\tilde{\alpha}_3^2(8\pi Pr_0^4 + 3Q^2)\right) + 54\tilde{\alpha}_2\tilde{\alpha}_3^3\tilde{\alpha}_2^3r_0^2 + 81\tilde{\alpha}_3^4\tilde{\alpha}_2^3\right)^{-1}$$

Figures 7 and 8 show the behavior of Helmholtz free energy versus r_o for different values of correction coefficient b and coupling constants of the regularized Lovelock theory $\tilde{\alpha}_2$ and $\tilde{\alpha}_3$. One can see that the influence of correction coefficient b is significant for large BH. The Helmholtz free energy becomes negative for large values r_o for all the values of correction coefficient. The Helmholtz free energy increases with increasing values of coupling

constants. Moreover, the coupling constants makes the Helmholtz free energy positive for higher values which mean it makes the BH stable and more work can be extracted from the system for higher values of the coupling constants. Moreover, when the Helmholtz free energy reaches to minimum value for $r_o \rightarrow 0$, the system shifts toward equilibrium state and no further work can be extracted.

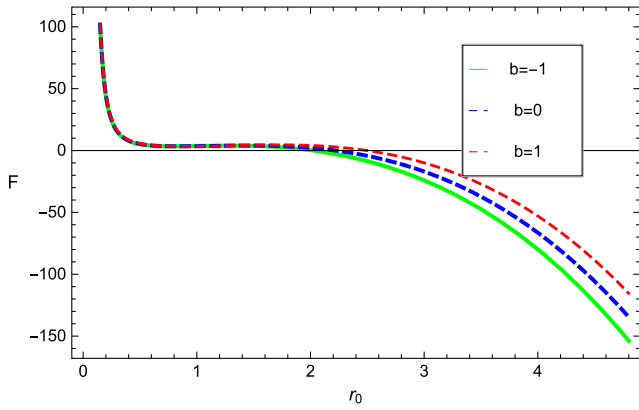


FIG. 7. Plot of Helmholtz free energy F versus r_0 for BH in regularized Lovelock theory.

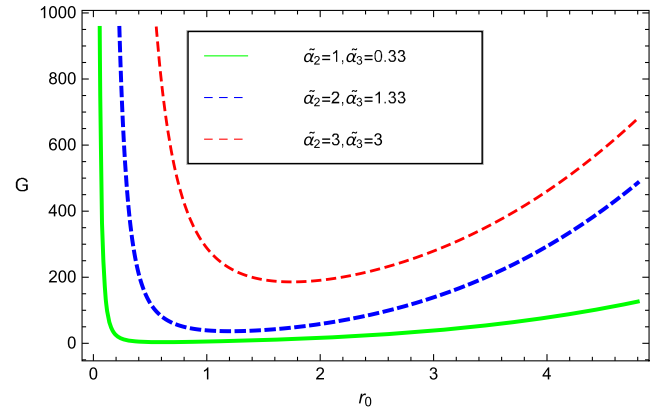


FIG. 10. Plot of Gibbs free energy G versus r_0 for BH in regularized Lovelock theory.

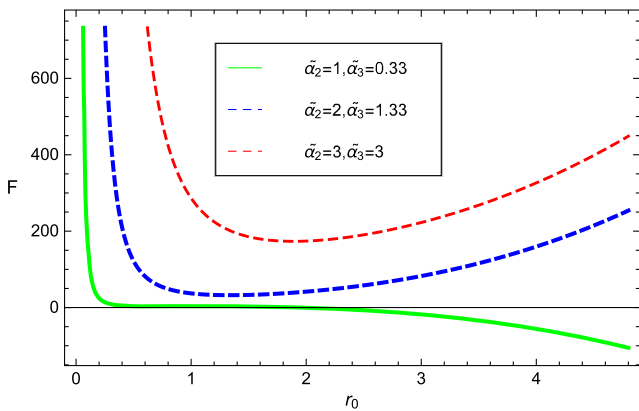


FIG. 8. Plot of Helmholtz free energy F versus r_0 for BH in regularized Lovelock theory.

Figures 9 and 10 demonstrate the behavior of Gibbs free energy of BH in regularized Lovelock theory for different values of correction coefficient b and coupling constants $\tilde{\alpha}_2$ and $\tilde{\alpha}_3$ respectively. For both the plots, Gibbs free energy is positive which yield nonspontaneous reactions which occur

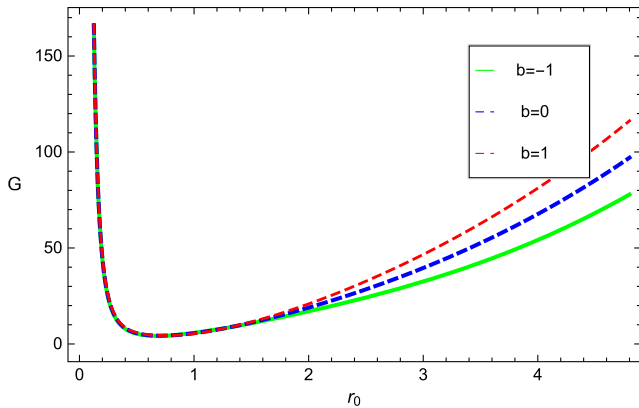


FIG. 9. Plot of Gibbs free energy G versus r_0 for BH in regularized Lovelock theory.

with outside source of energy. For all the values of correction coefficient and coupling constants Gibbs free energy is positive, which shows global stability of the BHs in Lovelock theory. The influence of the correction coefficient is significant for large BHs while the impact of coupling constants is significant throughout the horizon radius. The Gibbs free energy is also helpful to find out the phase transition points which exist at extreme values of Gibbs energy. The existence of extreme values in Gibbs free energy implies that phase transitions occurs in these type of BHs.

Figures 11 and 12 show the specific heat of BH in regularized Lovelock theory for different values of correction coefficient b and coupling constants $\tilde{\alpha}_2$ and $\tilde{\alpha}_3$, respectively. The regions with $C_V > 0$ represents the local stability of BH while $C_V < 0$ shows the local instability. The influence of coupling constants is significant because it makes the BH stable as can be seen for the plot Fig. 12. The negative correction coefficient $b = -1$ makes the specific heat of BHs in Lovelock theory more positive as compared to $b = 0, 1$ which means BH becomes more stable for negative correction coefficient.

The JT expansion is an isenthalpic process in which we study the change of temperature of the fluid under expansion.

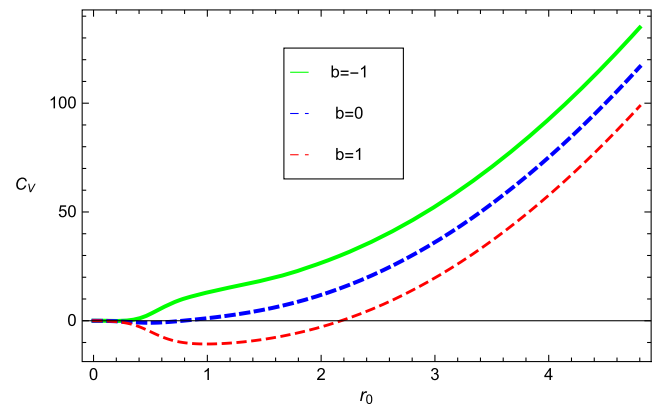


FIG. 11. Plot of specific heat C_V versus r_0 for BH in regularized Lovelock theory.

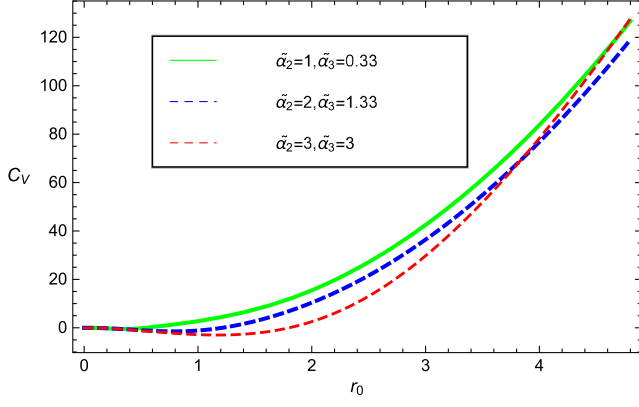


FIG. 12. Plot of specific heat C_V versus r_0 for BH in regularized Lovelock theory.

The change depend upon the JT coefficient which is given by [71]

$$U_{JT} = \left(\frac{\partial T}{\partial P} \right)_H. \quad (35)$$

This coefficient help us to find the heating and cooling phase. $U_{JT} = 0$ gives the inversion temperature T_i which is important point of temperature form which the temperature changes from cooling to heating or heating to cooling. It also defines the inversion pressure P_i and (T_i, P_i) gives the inversion transition point. By using generalized first law of BH thermodynamic and isenthalpic nature of the process one can rewrite the JT coefficient in term of the volume as [71]

$$U_{JT} = \left(\frac{\partial T}{\partial P} \right)_H = \frac{1}{C_p} \left[T \left(\frac{\partial V}{\partial T} \right)_p - V \right]. \quad (36)$$

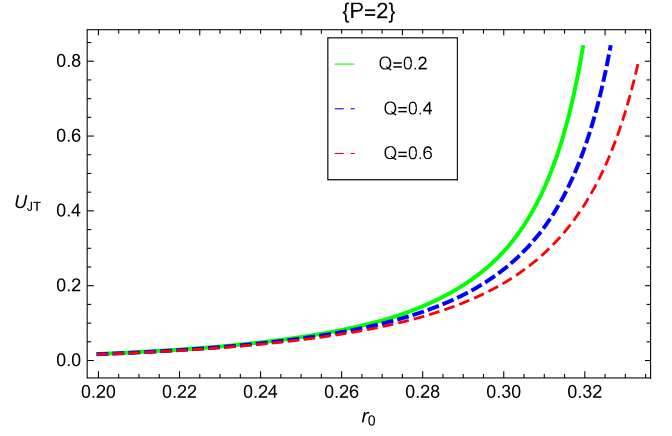


FIG. 13. Plot of JT coefficient for BH in regularized Lovelock theory.

Setting $U_{JT} = 0$ in the above equation yields the inversion temperature given by

$$T_i = V \left(\frac{\partial T}{\partial V} \right)_p. \quad (37)$$

Inversion temperature helps us to find the cold and hot phase in the T - P plane. The JT coefficient can also be written as follow [71]

$$U_{JT} = \left(\frac{\partial T}{\partial P} \right)_{M,q} = \left(\frac{\partial T}{\partial r_+} \right)_{M,q} \left(\frac{\partial r_+}{\partial P} \right)_{M,q}. \quad (38)$$

Using the temperature and pressure of BH in regularized Lovelock theory, the JT coefficient turns out to be

$$\begin{aligned} U_{JT} = & -4\tilde{\alpha}_2^2\tilde{\alpha}_3^2r_0^3(2\tilde{\alpha}_2^5\tilde{\alpha}_3^3r_0^{10} + \tilde{\alpha}_2^4r_0^8((21\tilde{\alpha}_3 - 2)\tilde{\alpha}_2^3 + 72\pi\tilde{\alpha}_3^2P) - 27r_0^2(\tilde{\alpha}_2^3\tilde{\alpha}_3\tilde{\alpha}_3^2Q^2 + 7\tilde{\alpha}_2\tilde{\alpha}_3^3\tilde{\alpha}_2^3) \\ & + 3\tilde{\alpha}_2^3\tilde{\alpha}_3r_0^6((24\tilde{\alpha}_3 - 5)\tilde{\alpha}_2^3 - 72\pi\tilde{\alpha}_3^2P) - 27\tilde{\alpha}_2^2r_0^4(\tilde{\alpha}_2^2\tilde{\alpha}_3^2Q^2 - 3\tilde{\alpha}_3^3\tilde{\alpha}_2^3 + 3(\tilde{\alpha}_3)^2\tilde{\alpha}_2^3) \\ & - 162(\tilde{\alpha}_3)^4\tilde{\alpha}_2^3)/3\tilde{\alpha}_3\tilde{\alpha}_2^3(\tilde{\alpha}_2r_0^2 + 3b)^3(3r_0^2(\tilde{\alpha}_2^3\tilde{\alpha}_3^2Q^2 + \tilde{\alpha}_2\tilde{\alpha}_3^2\tilde{\alpha}_2^3) \\ & - 24\pi\tilde{\alpha}_2^3\tilde{\alpha}_3^2Pr_0^6 - (\tilde{\alpha}_2)^2\tilde{\alpha}_3\tilde{\alpha}_2^3r_0^4 + 9\tilde{\alpha}_3^3\tilde{\alpha}_2^3). \end{aligned} \quad (39)$$

Finally, the inversion temperature of BH (from which BH temperature changes the mode) turns out to be

$$\begin{aligned} T_i = & \frac{1}{36\pi(\tilde{\alpha}_3)(\tilde{\alpha}_2^3)((\tilde{\alpha}_2)r_0^2 + 3(\tilde{\alpha}_3))^4} \left[\frac{((\tilde{\alpha}_2)^2r_0^2 + 3(\tilde{\alpha}_3)(\tilde{\alpha}_3))}{(\tilde{\alpha}_2)r_0^2} (27(\tilde{\alpha}_2)^4(\tilde{\alpha}_3^2)Q^2r_0^4 - 27r_0^2((\tilde{\alpha}_2)^3(\tilde{\alpha}_3)(\tilde{\alpha}_3^2)Q^2 \right. \\ & - 2(\tilde{\alpha}_2)(\tilde{\alpha}_3)^3(\tilde{\alpha}_2^3)) + 3(\tilde{\alpha}_2)^3(\tilde{\alpha}_3)r_0^6((\tilde{\alpha}_2^3) \left(2 \left(\frac{((\tilde{\alpha}_2)r_0^2 + 3(\tilde{\alpha}_3))^2}{(\tilde{\alpha}_2)r_0^2} - 7 \right) + 360\pi(\tilde{\alpha}_3^2)P \right) \\ & \left. + 2(\tilde{\alpha}_2)^4r_0^8((\tilde{\alpha}_2^3) \left(\left(\frac{((\tilde{\alpha}_2)r_0^2 + 3(\tilde{\alpha}_3))^2}{(\tilde{\alpha}_2)r_0^2} - 1 \right) + 36\pi(\tilde{\alpha}_3^2)P \right) + 81(\tilde{\alpha}_3)^4(\tilde{\alpha}_2^3)) \right]. \end{aligned}$$

Figures 13–15 show the behavior of JT coefficient for increasing values of charge of BH in regularized Lovelock theory. The zero of JT coefficient is important point which

leads to the inversion temperature of the BH. The important result of these plots is that at the zero of JT coefficient the influence of charge remains negligible and U_{JT} always

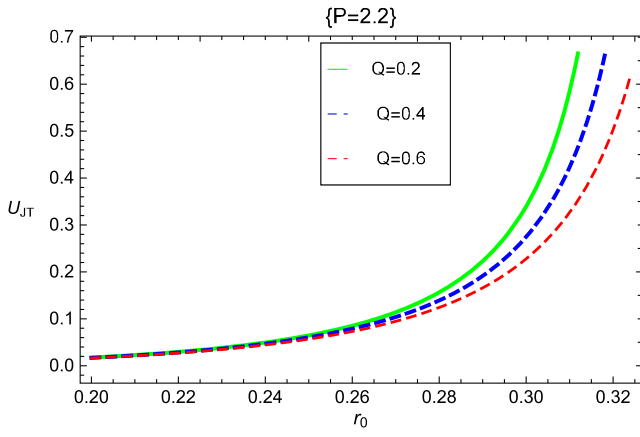


FIG. 14. Plot of JT coefficient for BH in regularized Lovelock theory.

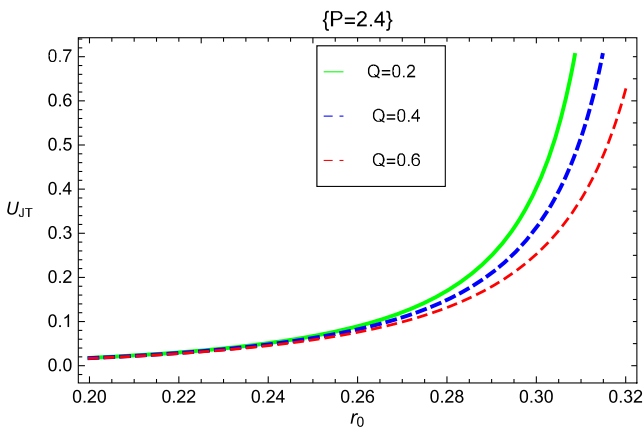


FIG. 15. Plot of JT coefficient for BH in regularized Lovelock theory.

remains positive which indicate that the expansion leads to cooling process. Figures 16–18 represent the inversion temperature T_i and inversion pressure P_i for increasing values of charge. It can be seen from the figure that the inversion curves are not closed and only one lowest

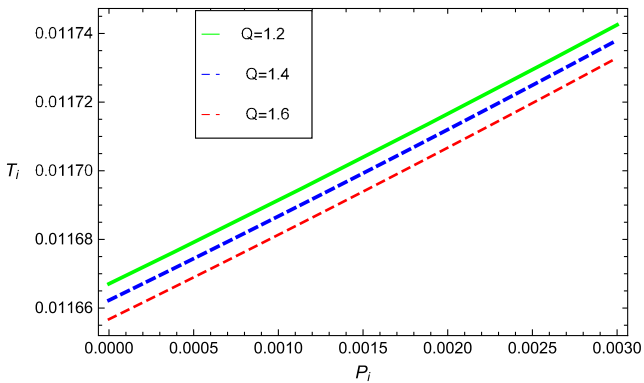


FIG. 16. Inversion curves $T_i - P_i$ for the heating and cooling regions for $(\tilde{\alpha}_3 > \tilde{\alpha}_2 > \tilde{\alpha}_2^3 > \tilde{\alpha}_3^2)$.

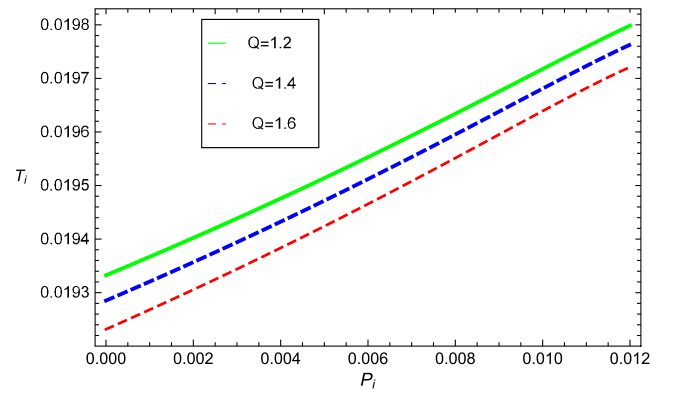


FIG. 17. Inversion curves $T_i - P_i$ for the heating and cooling regions for $(\tilde{\alpha}_3 > \tilde{\alpha}_2^3 > \tilde{\alpha}_2 > \tilde{\alpha}_3^2)$.

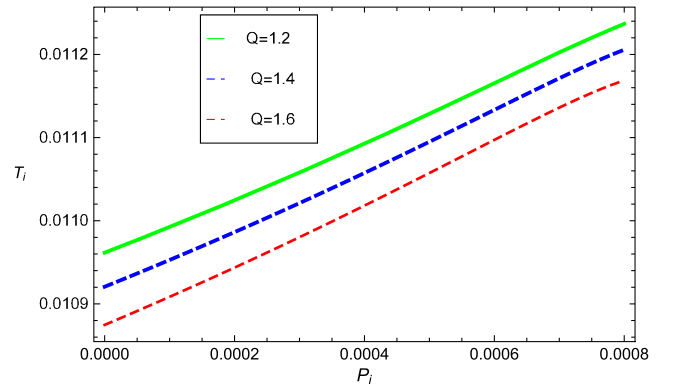


FIG. 18. Inversion curves $T_i - P_i$ for the heating and cooling regions for $(\tilde{\alpha}_3 > \tilde{\alpha}_3^2 > \tilde{\alpha}_2^3 > \tilde{\alpha}_2)$.

inversion curve is comparable with van der Waals fluids. The inversion temperature is inversely related with the charge of BH and it is used to separate the cooling and heating regimes. In all the three trajectories the position of inversion point (T_i, P_i) shifts to the higher values with increase in charge Q of the BH.

Figures 19–21 represent the isenthalpic curves with constant mass/enthalpy of BH in regularized Lovelock

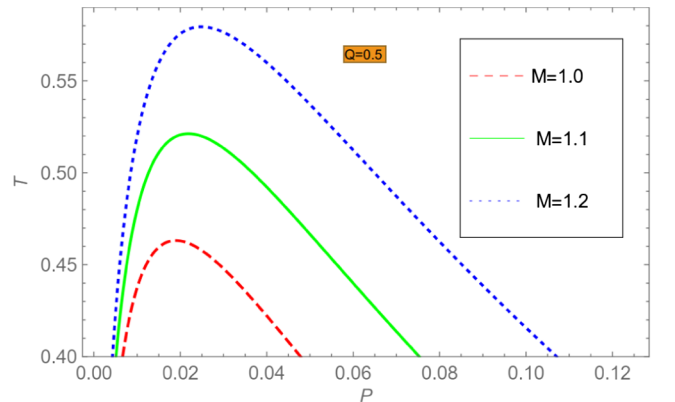


FIG. 19. Isenthalpic curves in $T - P$ plane with increasing values of M for BH in regularized Lovelock theory.

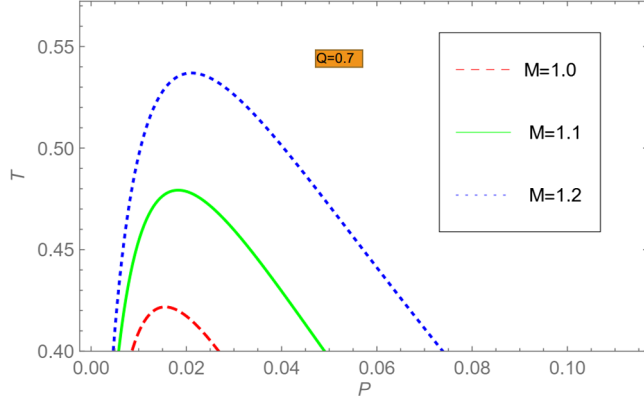


FIG. 20. Isenthalpic curves in T - P plane with increasing values of M for BH in regularized Lovelock theory.

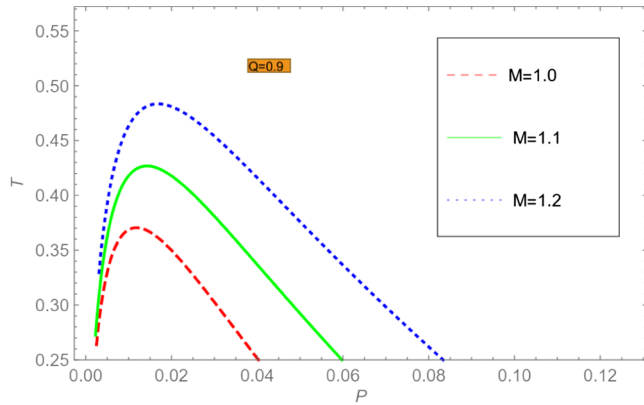


FIG. 21. Isenthalpic curves in T - P plane with increasing values of M for BH in regularized Lovelock theory.

theory in T - P plane. The inversion curves along with isenthalpic curves describe the cooling and heating regions. The inversion curves splits the plane of isenthalpic curves into two regions. The left side portion of inversion curve represents warm phase because the temperature increases there and the right side portion of curves represent cooling process. In order to discriminate the cooling / heating phases one can also check the sign of the slope of the isenthalpic curves. In the cooling region the slope remains positive and it turns to negative in the heating phase. Inversion curves play the role of barrier between the heating and cooling regimes.

V. CONCLUSION

The most basic thermodynamic quantity is enthalpy rather than internal energy due to non independence of volume and entropy of AdS BHs. Using this statement, we provided the general formalism for the line element of RTG and specific forms in different phase spaces for AdS BH in Einstein-Maxwell-scalars theory. We find out that the

curvatures in different spaces are same and positive, which indicate that it contains repulsive interactions between BH molecules in Einstein-Maxwell-scalars theory. In addition with no AdS background $P = 0$, curvature becomes zero which represents that the BH in Einstein-Maxwell-scalars theory with no AdS background is Ruppeiner flat.

We discussed the thermal stability of AdS BH in Einstein-Maxwell-scalars theory in the presence of thermal fluctuations. We observed that Helmholtz free energy increases with increasing values of momentum relaxation parameter β , which means more work can be extracted from the system for higher values of parameter β . For $\beta = 0$, the Helmholtz free energy becomes zero which shows the equilibrium state and no further work can be extracted without momentum relaxation. We also analyzed that for increasing values of the momentum relaxation parameter, the positive Gibbs free energy corresponds to nonspontaneous reactions which occurs with outside source of energy and BH remains globally stable. For all the values (positive and negative) of correction coefficient b the Gibbs free energy becomes negative which show global instability. We concluded that the momentum relaxation parameter β increases the thermal stability of the BH.

We also discussed the thermal corrected thermodynamics of BH in regularized Lovelock theory. We observed that the coupling constants of regularized Lovelock theory make the Helmholtz free energy positive for higher values which means BH become stable and useful work can be extracted from the system for higher values of the coupling constants. Moreover, when the Helmholtz free energy reaches to minimum value for $r_0 \rightarrow 0$, the system shifts toward equilibrium state and no further work can be extracted. We also observed that Gibbs free energy is positive for all the values of correction coefficient and coupling constants, which show that BHs in Lovelock theory are globally stable. We find out that the influence of coupling constants is significant for the local stability of the BHs. The negative correction coefficient $b = -1$ makes the specific heat of BHs in Lovelock theory more positive as compare to $b = 0, 1$ which means BH becomes more stable for negative correction coefficient. We also studied the JT expansion for static BH in regularized Lovelock theory. In order to discuss the change in temperature for the considered BH, we obtained the relations for JT coefficient, inversion and isenthalpic curves. We found out that the inversion curve split the cooling and heating regions and it works as barrier between the heating and cooling regimes.

ACKNOWLEDGMENTS

Shahid Chaudhary and Abdul Jawad would like to acknowledge HEC, Islamabad, Pakistan for its financial support through the Indigenous 5000 Ph.D. Fellowship Project Phase-II, Batch-V.

- [1] S. Hawking, *Commun. Math. Phys.* **43**, 199 (1975).
- [2] J. D. Bekenstein, *Phys. Rev. D* **7**, 2333 (1973).
- [3] S. W. Wei and Y. X. Liu, *Phys. Rev. Lett.* **115**, 111302 (2015).
- [4] R. G. Cai and J. H. Cho, *Phys. Rev. D* **60**, 067502 (1999).
- [5] J. L. Zhang, R. G. Cai, and H. W. Yu, *J. High Energy Phys.* **02** (2015) 143.
- [6] J. L. Zhang, R. G. Cai, and H. W. Yu, *Phys. Rev. D* **91**, 044028 (2015).
- [7] H. S. Liu, H. Lu, M. X. Luo, and K. N. Shao, *J. High Energy Phys.* **12** (2010) 054.
- [8] K. Bhattacharya, S. Dey, B. R. Majhi, and S. Samanta, *Phys. Rev. D* **99**, 124047 (2019).
- [9] D. Kastor, S. Ray, and J. Traschen, *Classical Quant. Grav.* **26**, 195011 (2009).
- [10] B. P. Dolan, *Classical Quant. Grav.* **28**, 125020 (2011).
- [11] B. P. Dolan, *Classical Quant. Grav.* **28**, 235017 (2011).
- [12] D. Kubiznak and R. B. Mann, *J. High Energy Phys.* **07** (2012) 033.
- [13] D. Kubiznak, R. B. Mann, and M. Teo, *Classical Quant. Grav.* **34**, 063001 (2017).
- [14] A. Singh, A. Ghosh, and C. Bhamidipati, *Front. Phys.* **9**, 631471 (2021).
- [15] S. W. Wei, Y. X. Liu, and R. B. Mann, *Phys. Rev. Lett.* **123**, 071103 (2019).
- [16] S. W. Wei, Y. X. Liu, and R. B. Mann, *Phys. Rev. D* **100**, 124033 (2019).
- [17] S. W. Wei and Y. X. Liu, *Phys. Lett. B* **803**, 135287 (2020).
- [18] R. B. Mann and S. N. Solodukhin, *Nucl. Phys.* **B523**, 293 (1998).
- [19] A. J. M. Medved and G. Kunstatter, *Phys. Rev. D* **60**, 104029 (1999).
- [20] B. Pourhassan and M. Faizal, *Europhys. Lett.* **111**, 40006 (2015).
- [21] V. P. Frolov, W. Israel, and S. N. Solodukhin, *Phys. Rev. D* **54**, 2732 (1996).
- [22] B. Pourhassan, M. Faizal, S. Upadhyay, and L. A. Asfar, *Eur. Phys. J. C* **77**, 555 (2017).
- [23] K. Nozari and S. H. Mehdipour, *Int. J. Mod. Phys. A* **21**, 4979 (2006).
- [24] H. Moradpour, Y. Heydarzade, C. Corda, A. H. Ziaie, and S. Ghaffari, *Mod. Phys. Lett. A* **34**, 1950304 (2019).
- [25] H. Moradpour, A. Dehghani, and M. T. M. Sabet, *Mod. Phys. Lett. A* **30**, 1550207 (2015).
- [26] H. Moradpour *et al.*, [arXiv:2106.00378](https://arxiv.org/abs/2106.00378).
- [27] G. G. L. Nashed and K. Bamba, *Prog. Theor. Exp. Phys.* **2020**, 043E05 (2020).
- [28] G. G. L. Nashed and K. Bamba, *Phys. Rev. D* **101**, 044029 (2020).
- [29] R. Ali, K. Bamba, and S. A. A. Shah, *Symmetry* **11**, 631 (2019).
- [30] G. G. L. Nashed and K. Bamba, *Entropy* **23**, 358 (2021).
- [31] A. Cisterna, S. Hu, and X. M. Kuang, *Phys. Lett. B* **797**, 134883 (2019).
- [32] T. Kaluza, *Int. J. Mod. Phys. D* **27**, 1870001 (2018).
- [33] J. Martin and J. Yokoyama, *J. Cosmol. Astropart. Phys.* **01** (2008) 025.
- [34] P. V. Nieuwenhuizen, *Phys. Rep.* **68**, 189 (1981).
- [35] C. A. R. Herdeiro, E. Radu, N. Sanchis-Gual, and J. A. Font, *Phys. Rev. Lett.* **121**, 101102 (2018).
- [36] P. G. Fernandes, C. A. Herdeiro, A. M. Pombo, E. Radu, and N. Sanchis-Gual, *Classical Quant. Grav.* **36**, 134002 (2019).
- [37] J. L. Blazquez-Salcedo, C. A. R. Herdeiro, J. Kunz, A. M. Pombo, and E. Radu, *Phys. Lett. B* **806**, 135493 (2020).
- [38] O. Okcu and A. Ekrem, *Eur. Phys. J. C* **78**, 123 (2018).
- [39] M. Chabab, H. El Moumni, S. Iraoui, K. Masmar, and S. Zhizeh, *Lett. High Energy Phys.* **1**, 05 (2018).
- [40] J.-X. Mo, G.-Q. Li, S.-Q. Lan, and X.-B. Xu, *Phys. Rev. D* **98**, 124032 (2018).
- [41] Q. S. Lan, *Phys. Rev. D* **98**, 084014 (2018).
- [42] M. X. Jie and L. Q. Gu, *Classical Quant. Grav.* **37**, 045009 (2020).
- [43] Y. M. Davood, H. Arezoo, and O. Okcu, *Phys. Lett. B* **795**, 521 (2019).
- [44] C. Adolfo, H. Q. Shi, and K. M. Xiao, *Phys. Lett. B* **797**, 134883 (2019).
- [45] R. A. Konoplya and A. Zhidenko, *Phys. Rev. D* **101**, 084038 (2020).
- [46] G. S. Pedro, *Phys. Lett. B* **805**, 135468 (2020).
- [47] A. Jawad, *Classical Quant. Grav.* **37**, 185020 (2020).
- [48] M. Yasir, K. Bamba, and A. Jawad, *Int. J. Mod. Phys. D* **30**, 2150068 (2021).
- [49] M. U. Shahzad, M. A. Nazir, and A. Jawad, *Phys. Dark Universe* **32**, 100828 (2021).
- [50] A. Jawad, M. Yasir, and S. Rani, *Mod. Phys. Lett. A* **35**, 2050298 (2020).
- [51] A. Jawad, S. Chaudhary, and K. Bamba, *Entropy* **23**, 1269 (2021).
- [52] A. Jawad, K. Jusufi, and M. U. Shahzad, *Phys. Rev. D* **104**, 084045 (2021).
- [53] G. Ruppeiner, *Phys. Rev. D* **78**, 024016 (2008).
- [54] G. Ruppeiner, *Am. J. Phys.* **78**, 1170 (2010).
- [55] G. Ruppeiner, *Springer Proc. Phys.* **153**, 179 (2014).
- [56] G. Ruppeiner, *Rev. Mod. Phys.* **67**, 605 (1995).
- [57] G. Ruppeiner, *Phys. Rev. D* **75**, 024037 (2007).
- [58] G. Ruppeiner, *Springer Proc. Phys.* **153**, 179 (2014).
- [59] G. Ruppeiner, *Am. J. Phys.* **78**, 1170 (2010).
- [60] S. W. Wei and Y. X. Liu, *Phys. Rev. Lett.* **115**, 111302 (2015).
- [61] S. W. Wei, Y. X. Liu, and R. B. Mann, *Phys. Rev. Lett.* **123**, 071102 (2019).
- [62] S. W. Wei, Y. X. Liu, and R. B. Mann, *Phys. Rev. D* **100**, 124033 (2019).
- [63] S. W. Wei and Y. X. Liu, *Phys. Lett. B* **803**, 135287 (2020).
- [64] Y. G. Miao and Z. M. Xu, *Phys. Rev. D* **98**, 044001 (2018).
- [65] Y. Bardoux, M. M. Caldarelli, and C. Charmousis, *J. High Energy Phys.* **05** (2012) 054.
- [66] N. Iizuka and K. Maeda, *J. High Energy Phys.* **07** (2012) 129.
- [67] T. Andrade and B. Withers, *J. High Energy Phys.* **05** (2014) 101.
- [68] Z. M. Xu, B. Wu, and W. L. Yang, *Eur. Phys. J. C* **80**, 997 (2020).
- [69] D. Glavan and L. Chunshan, *Phys. Rev. Lett.* **124**, 081301 (2020).
- [70] R. A. Konoplya and A. Zhidenko, *Phys. Rev. D* **101**, 084038 (2020).
- [71] C. Li, P. He, and P. L. Deng, *Gen. Relativ. Gravit.* **52**, 50 (2020).